Check for updates

# Flood Risk Assessment of Traditional Adobe Buildings: Analysis of Case Studies in the River Ebro Basin, Spain

Francesca Trizio(✉), F. Javier Torrijo Echarri, Camilla Mileto, and Fernando Vegas

Research Centre PEGASO, Universitat Politècnica de València, Camí de Vera S/N, 46022 Valencia, Spain

fratri@upvnet.upv.es

**Abstract.** Earthen masonry is a historic construction technique widespread in the river Ebro basin (Spain). These masonry walls are made of small earthen blocks, such as adobes [1]. Throughout history frequent floods of the river Ebro have threatened the integrity of earthen masonry construction. Due to climate change, this region is undergoing an increase in the severity and frequency of flood events, causing considerable losses to architectural heritage [2]. According to various studies, earth as a building material has hygroscopic characteristics which influence its resistance to water [3]. The devastating effects of flood events on historic structures due to changes in the interaction between subsoil and foundations include damage to the superstructure [4]. This research proposes a flood risk assessment methodology following a component-based modelling framework. The susceptibility to floods of the building components is evaluated, considering the material, structural and morphological characteristics [5]. The conservation state of the assets is also considered, analysing material weathering, damage, and crack patterns. The individual parameters involved in the assessment have been weighted in order to ensure significant results. The methodology has been applied to a group of municipalities located in the floodplain of the middle course of the river Ebro, and this research aims to carry out a flood risk assessment of adobe buildings on a local scale. Different risk levels have been found depending on the specific characteristics and conservation state of individual assets. The correlation between structural damage and flood effects is examined to identify the origin of damage and recurring crack patterns. Finally, mitigation strategies are discussed in relation to the importance of the conservation of architectural heritage and vernacular construction traditions.

**Keywords:** Floods · Risk Assessment · Earthen Architecture · Adobe · Vernacular Heritage

## 1 Introduction

Floods can be considered the most common natural risk worldwide. According to the Emergency Event Database (EM-DAT), in the last four decades floods have been the cause of most disasters, accounting for 33% of catastrophic events recorded between


Y. Endo and T. Hanazato (Eds.): SAHC 2023, RILEM Bookseries 46, pp. 1067–1079, 2024.
https://doi.org/10.1007/978-3-031-39450-8_87

1980 and 1999 and 44% of those observed between 2000 and 2019 [6]. In recent years, several flooding events have occurred in Spain, with an average of ten severe episodes per year [7, 8]. Climate change has considerably increased the risk of flooding in this region, exacerbating the alternation of dry periods and heavy rains [2]. Flood hazard in Spain varies according to the geomorphological and climate characteristics of the basin.

The Ebro Basin, in the northeast of the Iberian Peninsula, is the largest river basin in Spain, with a total area of 85,534 $km^2$ (17% of the Spanish peninsular territory). It is drained by the Ebro River which runs in a northwest-southeast direction, from the Cantabrian mountains to the Mediterranean Sea (Fig. 1a). The flooding of the Ebro in its lower-middle course is associated with long-term frontal rainfall. The consequences of these episodes affect the area's population and cultural heritage. Part of this heritage, earthen traditional architecture, bears witness to an "architecture without architects" [9] which has managed to survive the passage of time thanks to constant modification and adaptation to the conditions of the environment. This is the case of adobe masonry walls, one of the region's most widespread earthen construction techniques. Recent studies have collected information on these constructions, studying their characteristics and the material degradation processes affecting them [1, 10].

In general, historic buildings are affected by the effects of flooding, which causes visible damage to superstructures [11] and foundations due to changes in stresses and deformations of the ground [4]. In the case of built earthen heritage, its intrinsic hygroscopicity increases the adverse effects of the action of water, affecting its mechanical characteristics and causing the structure to collapse [12, 13]. Flood risk reduction in heritage contexts is considered crucial for risk management. Given the impossibility of eliminating risk, strategies for flood risk reduction aim to keep flood damage below an acceptable threshold. Hence, several studies have developed different methodologies to assess the flood vulnerability [14, 15] and risk [16–18] of heritage buildings.

However, while most studies focus mainly on stone and brick as traditional materials, very few research earthen architecture and floods [5, 19, 20]. This study aims to bridge this gap by presenting an approach designed to assess earthen masonry on a local scale. Different spatial scales require individual assessment methods, depending on their characteristics and the application of the assessment [21]. In this study, the local scale refers to a small area such as a town or small settlement. The methodology is applied to a significant sample of traditional adobe buildings in two municipalities of the Ebro Basin: Torres de Berellén and Boquiñeni (Zaragoza, Spain). The town of Boquiñeni lies on a river terrace (Fig. 1b) that narrows naturally upstream but ends in a meander downstream near the town. The village of Torres de Berellén is located on a slope (Fig. 1c) above two river terraces, with most of the town sitting on the upper terrace (215 m a.s.l.) and the northeast area on the lower terrace (211 m a.s.l.). Over time, both municipalities suffered the consequences of catastrophic floods, with significant peak flows which in some cases exceeded 4000 $m^3/s$ [22]. The two most recent floods, in 2015 and 2018, caused extensive damage as water surrounded the towns, completely isolating them. Both municipalities are currently classified as flood-prone towns and included in the Areas of Significant Potential Flood Risk of the Middle Ebro [23].

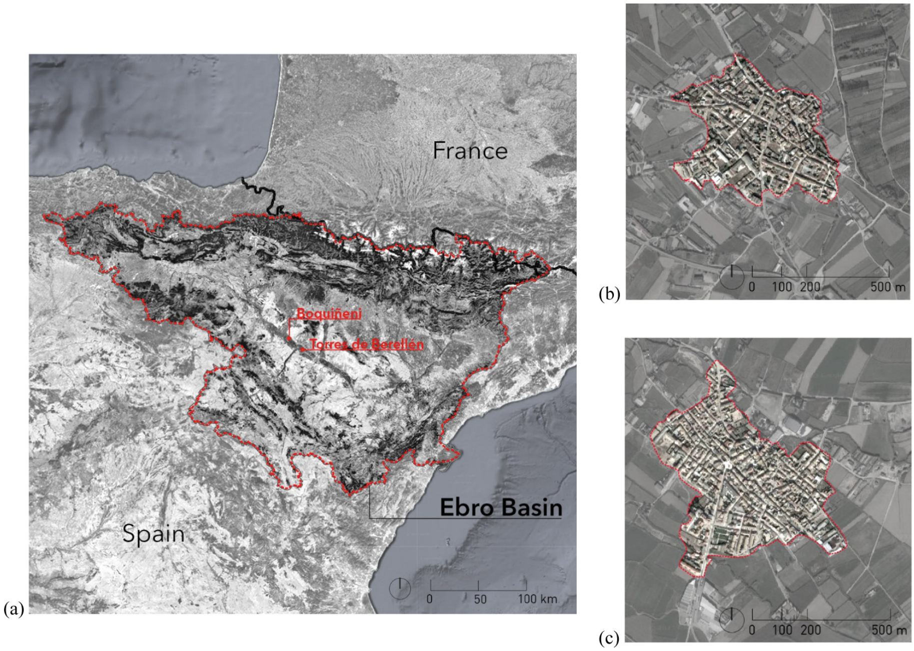


**Fig. 1.** Site maps of the case study area: (a) Ebro Basin; (b) Boquiñeni; (c) Torres de Berellén.

## 2 Risk Assessment Methodology

Three components generally govern flood risk: hazard, exposure, and vulnerability [24]. Hazard measures the frequency and intensity of flooding; exposure represents the assets at risk, and vulnerability quantifies the susceptibility of the assets or the level of expected damage.

The assessment methodology of this study is based on a multi-parameter approach divided into three steps: exposure dataset generation, vulnerability index modelling, and risk index quantification. During the first phase of the research, an exposure dataset was generated, implementing the information of flood hazard maps and traditional earthen architecture dataset. This paper does not discuss exposure dataset generation as it forms part of a previous research phase. Hazard maps developed by the Ebro Hydrographic Confederation were used to define flood hazard levels [25]. These maps are based on the guidelines set out in European Directive 2007/EC/60 on the assessment and management of flood risks [26] and correspond to low hazard (10-year return period), medium hazard (100-year return period), and extreme events (500-year return period). Seven hazard levels are defined by water depth, from a minimum level below 0.20 m to a maximum of more than 2 m. For the purposes of selecting the research area, the distribution maps of traditional earthen architecture in the Iberian Peninsula developed as part of the SOStierra project were used [27]. These maps were obtained following the cataloguing of earthen constructions in 618 sites in the Iberian Peninsula. The data acquired through fieldwork sessions was used to complete previous information. The location of the buildings in UTM coordinates and their characteristics were identified in these sessions. GIS technology was used for the superimposition of hazard maps and the point layer created from the data collected in situ, resulting in an exposure map of the assets-at-risk.

The second step of the research focused on modelling a flood vulnerability index. This index quantifies the vulnerability of individual assets. A component-based assessment methodology considers the characteristics and susceptibility of earthen buildings, expressing the degree of adverse effects of flooding that an asset may endure. The vulnerability index is calculated by assigning a susceptibility factor (SF) to the characteristics of the building on a scale from 1 (low susceptibility) to 5 (high susceptibility). Weighting factors (W) are applied to the susceptibility factors in order to obtain significant results. The weights were calculated using the Delphi Method [28]. A group of 43 experts selected from different fields (29 architects, 4 experts in heritage conservation, 8 engineers, 1 geotechnical engineer, 1 sociologist) was asked to complete a survey evaluating the influence of individual susceptibility factors on global building behaviour on a scale from 0 to 10. The average value of each weight was obtained by applying the Chauvenet criterion [19]. Table 1 shows the susceptibility factors and their weights used to calculate the vulnerability index.

**Table 1.** Earthen architecture susceptibility factors (SF) and weighting factors ($w_S$).

| Characteristic | $w_s$ | SF | Characteristic | $w_s$ | SF |
|---|---|---|---|---|---|
| Urban location | 0.8 | | Construction technique | 0.6 | |
| - With Basement | | 5 | - Homogeneous adobe | | 5 |
| - Below ground | | 4 | - Supplemented adobe | | 3 |
| - Ground level | | 3 | - Mixed adobe | | 1 |
| - Above ground | | 1 | | | |
| - Sloping ground | | 3 | | | |
| Footprint [m$^2$] | 0.4 | | Mortar joints | 0.6 | |
| - 0–50 | | 5 | - Earth | | 5 |
| - 50–250 | | 3 | - Lime | | 4 |
| - >500 | | 1 | - Reed in joints | | 4 |
| Number of floors | 0.4 | | - Bricks in joints | | 2 |
| - 1 | | 1 | - Stone in joints | | 2 |
| - 2–3 | | 3 | - Wood in joints | | 3 |
| - 4–5 | | 5 | | | |
| Building type | 0.4 | | Plinth | 0.7 | |
| - Freestanding | | 5 | - No plinth | | 5 |
| - End of block | | 4 | - Masonry | | 3 |
| - On a corner | | 3 | - Ashlar | | 1 |
| - Detached | | 1 | - Brick | | 2 |
| Additional protection | 0.5 | | Rendering | 0.5 | |
| - Yes | | 1 | - No rendering | | 5 |
| - No | | 5 | - Earth | | 4 |
| | | | - Earth and lime | | 2 |
| | | | - Earth and fibres | | 3 |
| | | | - Lime | | 1 |
| | | | - Gypsum | | 3 |

The scale of a construction (footprint and number of floors) influences its capacity to resist water drag. This capacity is also conditioned by position on the ground (urban level) and building type. Moreover, the construction technique used in an earthen wall determines its resistance to the action of water. Adobe masonry walls respond better to rising damp than rammed earth, as mortar joints block water movement [12]. However, this quality can be reduced or increased depending on the material of the mortar joints. Capillarity can be reduced by the presence of a plinth, depending on the absorption rate of the material used. The outer surface of a wall significantly influences the water absorption rate, depending on the hygrometric characteristic and homogeneity of the rendering. The state of conservation of a building is fundamental for evaluating its vulnerability. Considerably deteriorated assets may be more susceptible to the effects of floods. Cracks, erosion processes, and rising damp can increase susceptibility, facilitating moisture infiltration. Thus, damage-weighted factors are implemented in the vulnerability index modelling (see Table 2).

**Table 2.** Damage factors (DF) and weights (wd).

| Damage | $w_d$ | DF | Damage | $w_d$ | DF |
|---|---|---|---|---|---|
| Wall erosion | 0.7 | | Structural damages | 1 | |
| - Absent | | 1 | - Absent | | 1 |
| - Superficial | | 2 | - Hair crack | | 3 |
| - In the joints | | 3 | - Minor crack | | 4 |
| - Diffuse | | 4 | - Deep crack | | 5 |
| - Volumetric loss | | 5 | | | |
| Rendering erosion | 0.5 | | Rising damp | 0.6 | |
| - Absent | | 1 | - Absent | | 1 |
| - Superficial | | 2 | - Present | | 5 |
| - Partial | | 3 | | | |
| - Considerable | | 4 | | | |
| - Heavy | | 5 | | | |
| Plinth erosion | 1 | | Wall saturation | 0.8 | |
| - Absent | | 1 | - Absent | | 1 |
| - Superficial | | 3 | - Present | | 5 |
| - In the joints | | 4 | | | |
| - Volumetric loss | | 5 | | | |

The flood vulnerability index (FVI) for each asset is obtained using Eq. (1):

$$FVI_i = \frac{\sum_{i=1}^{n}(SF_i ws_i)}{\sum w_s}\frac{\sum_{i=1}^{n}(DF_i wd_i)}{\sum w_d} \quad (1)$$

The first term of the equation represents the intrinsic susceptibility of the building, where $SF_i$ is the susceptibility value of each characteristic of the $i$th asset, and $ws_i$ is the relative weight. The second term represents the structural and material damage, where $DF_i$ is the value assigned to each type of damage, and $wd_i$ is the associated weight. The index is expressed in a range between 1 and 10.

Depending on the degree of probability of the risk, the expected annual average damage due to flooding, also known as risk curve, is generally considered an adequate representation of the relationship between the probability of occurrence of the different events and their corresponding impact on the exposed elements [29]. Based on this risk formulation, flood risk is represented by the area under the curve. The risk index (RI) is calculated as an approximation of this area using Eq. (2) and (3):

$$RI_i = FVI[i] \cdot \Delta P_i \tag{2}$$

$$FVI[i] = \frac{FVI(p_i1) + FVI(P_i)}{2} \tag{3}$$

The term $\Delta Pi = |P_i - P_{i-1}|$ represents the probability of occurrence between two hazard scenarios, assumed as the inverse of their return period, and *FVI[i]* is the mean value of the vulnerability index of the *i*th asset associated with these hazard scenarios. The present study considers return periods of 10, 100, and 500 years for the assessment. The function $FVI(P_i)$ is obtained with Eq. (4):

$$FVI(P_i) = FVI_i \cdot h \tag{4}$$

The parameter *h* represents the influence of water depth associated with the return period. This parameter is established by dividing water depth values into four intervals (Table 3). According to numerous studies found in the available literature [8, 30, 31], depth-damage functions show an increase in damage of 20% for water depths of approximately 1 m. For depths between 1 and 2 m, an increase in damage of 40% is estimated, while water depths of more than 2 m result in an increase of 60% in damage to the structures.

**Table 3.** Water depth ranges and corresponding parameters.

| Water depth (m) | h |
|---|---|
| = 0 | 0 |
| 0– 1 | 1.2 |
| 1– 2 | 1.4 |
| ≥2 | 1.6 |

Finally, RI values corresponding to different return periods are normalised between 0 and 1 to obtain comparable values without distorting differences. Risk maps for both case studies are obtained by implementing the results in the attribute table of the GIS file.

## 3 Results and Discussion

The risk assessment approach proposed in this study has been applied to 53 adobe buildings, 38 of which are in Torres de Berellén and 15 in Boquiñeni (Fig. 2). These residential buildings are between 3 and 8 m high (one to three-story buildings). Generally, only the upper floors are used as a dwelling, while the ground floor is used for storage. All these assets are built with adobe walls 40 to 60 cm deep resting on brick plinths. On average the adobe blocks measure 17.5 × 7.5 cm, with 2 cm mortar joints.

(a) (b) (c)

**Fig. 2.** (a) Two-story adobe building in Torres de Berellén; (b) Single-story adobe building in Torres de Berellén; (c) Two-story adobe building in Boquiñeni.

Some considerations can be made regarding the effects of floods and land structures based on the observation and analysis of the assets. Walls exhibit several types of deterioration resulting from the direct and indirect effects of flooding. The percentage distribution graph in Fig. 3 shows the presence of erosion and detachment of the rendering in many assets (Fig. 4a), possibly caused by rising damp and dry-wet cycles. Generally, rising damp is not considered an influential factor in flood damage assessment. However, Kelman and Spence [32] demonstrated its relevance, as it can trigger indirect damage. During a flood, materials are quick to reach complete saturation, giving rise to changes to their physical and mechanical properties.

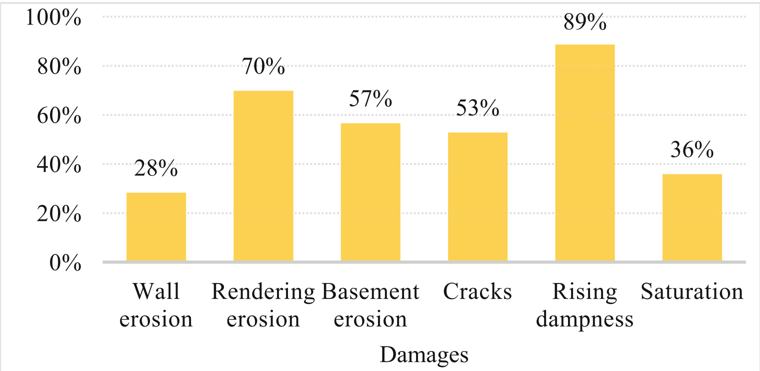


**Fig. 3.** Percentage distribution of damage.

Long-term effects of flooding can lead to structural damage such as cracks and deformation. More than half of the assets analysed display vertical and parabolic cracks possibly caused by rotations and subsidence (Fig. 4b). According to Herle et al. [4], flooding affects the foundation soil, changing its hydraulic state. Thus, cracks and deformations appear in the superstructure due to the increase in the hydraulic gradient, causing soil erosion, subsidence, and damage to the foundations of the buildings. Moreover, the vertical and parabolic crack patterns depend on the lack of transverse connection between walls, which are free to rotate or move independently.

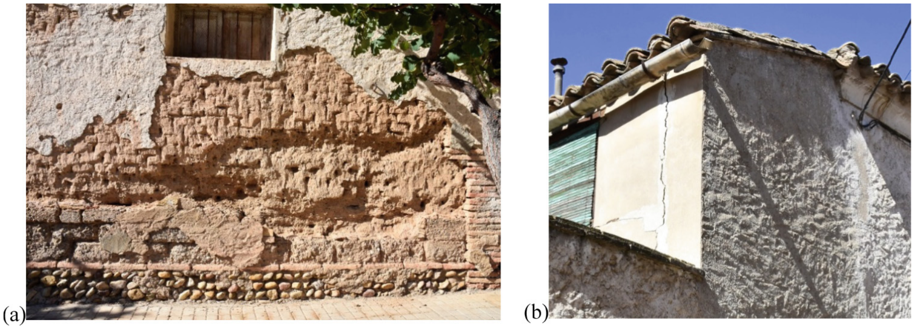

**Fig. 4.** (a) Wall and plinth erosion; (b) Vertical crack.

As mentioned previously, following an initial detailed analysis of the assets, the RI values were individually calculated based on the initial vulnerability assessment. Assets were inserted into a vector layer as points using UTM coordinates. The characteristics of the assets were added to the layer's attribute table, generating a dataset. The point layer was superimposed onto the hazard maps to obtain the water depth values for each asset.

For the 10-year return period, results were nil and omitted, as water does not affect the assets. Figure 5 shows the RI percentage distribution corresponding to 100- and 500-year return periods. A comparison of the graphs in Fig. 5 reflects a significant variation. The percentage distribution graph for the 500-year return period shows an increase of 9% and 2% in assets with RI values between 0.25–0.50 and 0.50–0.75, respectively. This variation is due to increased water depths for the 500-year return period hazard map.

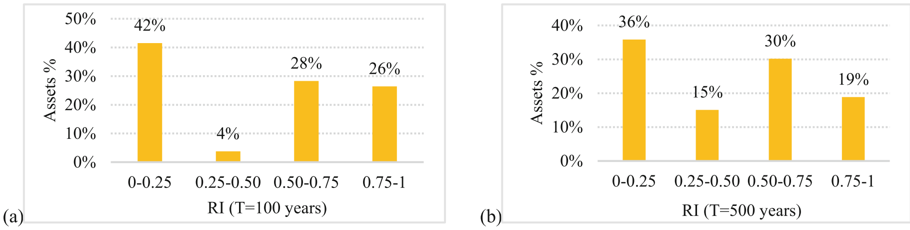


**Fig. 5.** (a) Percentage distribution graph of the RI values for a return period of 100 years. (b) Percentage distribution graph of the RI values for a return period of 500 years

Figure 6 represents the spatial distribution of the elements at risk for the considered return periods. The assets in Boquiñeni are more exposed to floods than those in Torres de Berellén as the potentially floodable area is larger.

Assessment results and risk maps are essential for prioritising further analyses, opening up the possibility of possible flood management strategies considering the available resources. However, these results should not be considered definitive for the implementation of risk mitigation measures. Instead, they constitute a starting dataset for identifying potentially at-risk assets that require more detailed analysis.

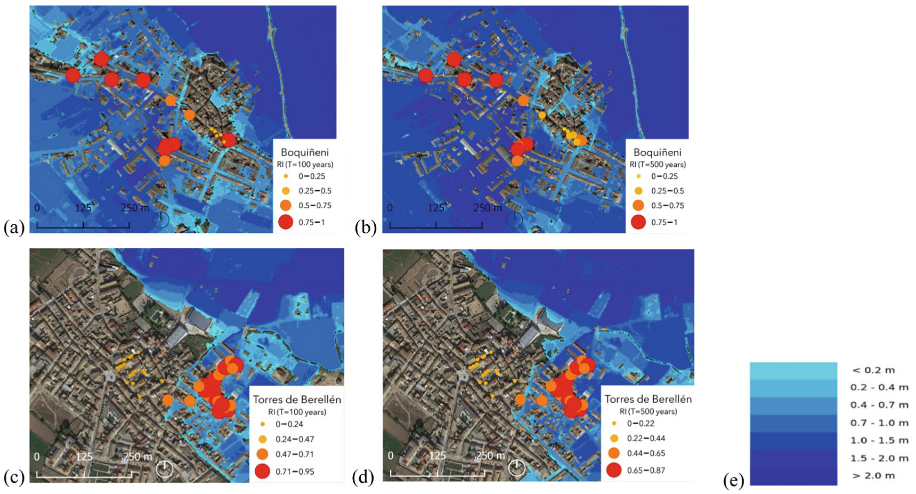


**Fig. 6.** Maps of RI values for earthen architecture exposed to fluvial flooding: (a) Boquiñeni, T = 100 years; (b) Boquiñeni, T = 500 years; (c) Torres de Berellén, T = 100 years; (d) Torres de Berellén T = 500 years; (e) water depth key.

Detailed information about the results is provided in Table 4. For readability, RI nil values are omitted. These values correspond to nil values of water depth. In some cases, nil RI values calculated for a probability of occurrence of 100 years increase greatly for a 500-year return period. As mentioned above, this increase mainly depends on the water depth coefficient. However, the value of the vulnerability index remains constant as it is only influenced by the characteristics of the masonry.

**Table 4.** Results of vulnerability and risk index values for traditional adobe buildings.

| ID | Latitude | Longitude | FVI | FVI (T = 100y) | FVI (T = 500y) | RI (T = 100y) | RI (T = 500y) |
|---|---|---|---|---|---|---|---|
| 1 | 660909.09 | 4624630.01 | 4.67 | 5.60 | 5.60 | 0.64 | 0.60 |
| 2 | 660966.52 | 4624627.404 | 4.31 | 5.17 | 5.17 | 0.60 | 0.55 |
| 3 | 661029.01 | 4624649.865 | 6.85 | 8.22 | 8.22 | 0.95 | 0.87 |
| 4 | 661013.67 | 4624642.042 | 3.98 | 4.77 | 4.77 | 0.55 | 0.51 |
| 5 | 661036.57 | 4624629.956 | 5.77 | 6.92 | 6.92 | 0.80 | 0.74 |
| 6 | 661041.07 | 4624626.05 | 3.82 | 4.59 | 4.59 | 0.53 | 0.49 |
| 7 | 661044.48 | 4624599.914 | 6.19 | 7.43 | 7.43 | 0.86 | 0.79 |
| 8 | 661066.83 | 4624604.832 | 6.40 | 7.68 | 7.68 | 0.88 | 0.82 |
| 10 | 661074.53 | 4624615.481 | 3.59 | 4.31 | 5.03 | 0.50 | 0.50 |
| 11 | 661058.91 | 4624610.741 | 4.13 | 4.95 | 4.95 | 0.57 | 0.53 |
| 12 | 661051.64 | 4624616.848 | 5.77 | 6.92 | 6.92 | 0.80 | 0.74 |
| 13 | 661006.88 | 4624655.991 | 6.39 | 7.67 | 7.67 | 0.88 | 0.81 |
| 14 | 661009 | 4624667.865 | 6.31 | 7.57 | 7.57 | 0.87 | 0.80 |

(*continued*)

**Table 4.** (*continued*)

| ID | Latitude | Longitude | FVI | FVI (T = 100y) | FVI (T = 500y) | RI (T = 100y) | RI (T = 500y) |
|---|---|---|---|---|---|---|---|
| 15 | 661031.59 | 4624682.764 | 5.31 | 6.37 | 7.43 | 0.73 | 0.73 |
| 16 | 661042.67 | 4624696.419 | 3.75 | 4.51 | 5.26 | 0.52 | 0.52 |
| 17 | 661050.19 | 4624705.737 | 3.79 | 4.55 | 5.31 | 0.52 | 0.52 |
| 18 | 661060.12 | 4624715.842 | 5.91 | 7.09 | 8.27 | 0.82 | 0.82 |
| 19 | 661073.45 | 4624733.522 | 4.24 | 5.09 | 5.94 | 0.59 | 0.59 |
| 20 | 661088.81 | 4624721.691 | 5.40 | 6.48 | 7.56 | 0.75 | 0.75 |
| 21 | 661078.86 | 4624712.586 | 4.20 | 5.04 | 5.87 | 0.58 | 0.58 |
| 22 | 660990.53 | 4624665.657 | 3.44 | 4.13 | 4.82 | 0.48 | 0.48 |
| 23 | 645132.87 | 4634295.956 | 6.14 | 7.37 | 8.60 | 0.85 | 0.85 |
| 24 | 645113.03 | 4634291.401 | 4.89 | 6.84 | 6.84 | 0.79 | 0.73 |
| 25 | 645109.89 | 4634282.382 | 5.42 | 7.58 | 7.58 | 0.87 | 0.81 |
| 26 | 645108.67 | 4634250.969 | 4.18 | 5.01 | 5.85 | 0.58 | 0.58 |
| 27 | 645283.22 | 4634307.281 | 5.65 | 6.78 | 6.78 | 0.78 | 0.72 |
| 28 | 645270.92 | 4634302.656 | 6.06 | 0.00 | 7.27 | 0.00 | 0.39 |
| 29 | 645261.55 | 4634321.57 | 6.35 | 0.00 | 7.61 | 0.00 | 0.40 |
| 30 | 645250.59 | 4634319.302 | 6.32 | 0.00 | 7.59 | 0.00 | 0.40 |
| 31 | 645176.66 | 4634375.843 | 4.64 | 5.57 | 0.00 | 0.64 | 0.30 |
| 32 | 645125.42 | 4634414.484 | 5.14 | 6.16 | 7.19 | 0.71 | 0.71 |
| 33 | 645051.27 | 4634470.475 | 5.46 | 6.55 | 7.65 | 0.75 | 0.75 |
| 34 | 644965.53 | 4634471.773 | 7.24 | 8.69 | 10.14 | 1.00 | 1.00 |
| 35 | 644860.02 | 4634483.385 | 6.01 | 7.21 | 7.21 | 0.83 | 0.77 |

This research proposes an innovative approach to the flood risk assessment of traditional adobe buildings. Application to a sample of adobe buildings provides information on the risk associated with this traditional construction typology. While most risk assessment models are based on economic analysis the approach followed here is based on the concepts set out in risk assessment theory, applied to vernacular heritage. However, the application of these models in the field of heritage is a much-debated issue, as the value of a heritage asset depends on intangible parameters such as artistic, historical, and commemorative value, which could not be subjected to exhaustive economic assessment. Therefore, the risk assessment index that considers the specific characteristics of traditional earthen buildings was structured, detailing the parameters according to materials and techniques. It should be noted that the evaluation of heritage buildings can entail a certain degree of uncertainty given the difficulty in obtaining information. This approach combines qualitative and quantitative methods to consider these issues. Risk assessment results form the basis for risk prevention measures. Prevention can include different strategies: legislation, mitigation, and citizen education. Plans, laws, and regulations such as sectoral regulations on water, territorial management, building, and urban planning aim to reduce the exposure and vulnerability of potentially at-risk assets. Unlike legislation that acts before a natural event occurs, mitigation measures try to reduce the impact of the flood at the time it happens. Depending on the context and risk level these measures can be structural or engineering, non-structural or management. In the case of traditional earthen architecture, conservation and restoration measures are crucial for reducing the vulnerability of buildings and increase their resilience. Establishing a framework of intervention criteria for damaged and deteriorated assets that consider the specific characteristics of traditional buildings is fundamental to preserving their values.

## 4 Conclusions

Floods are a frequent threat to earthen architectural heritage. It is essential to develop flood risk assessment studies to mitigate the adverse effects of flooding. The methodology proposed in this research focuses on analysing the characteristic elements of this architecture in order to define vulnerability parameters. In addition, water depth is entered into the calculation as the measure of the severity of flooding. Implementing the information in GIS maps is essential for generating a database that can be updated according to assets and environmental changes. Results obtained according to the probability of occurrence provide information on the risk levels of individual assets, highlighting those most at risk in order to carry out further assessments of the assets themselves. Future lines of research should focus on conservation and risk mitigation strategies to preserve the identity values of traditional architecture.

**Acknowledgements.** This work is part of the research project "Earthen architecture in the Iberian Peninsula: study of natural, social and anthropic risks and strategies to improve resilience" Risk-Terra (ref. RTI2018–095302-B-I00; main researchers: Camilla Mileto and Fernando Vegas), funded by the Spanish Ministry of Science, Innovation and University.

## References

1. Gómez-Patrocinio, F.J., Vegas López-Manzanares, F., Mileto, C., García-Soriano, L.: Techniques and characteristics of traditional earthen masonry walls: the case of Spain techniques and characteristics of traditional Earthen Masonry Walls: The Case of Spain. Int. J. Archit. Herit. **14**, 694–710 (2020). https://doi.org/10.1080/15583058.2018.1563238
2. Lastrada, E., Cobos, G., Torrijo, F.J.: Analysis of climate change's effect on flood risk. Case study of Reinosa in the Ebro river Basin. Water (Switzerland) **12** (2020). https://doi.org/10.3390/W12041114
3. Beckett, C.T.S., Jaquin, P.A., Morel, J.C.: Weathering the storm: A framework to assess the resistance of earthen structures to water damage. Constr. Build. Mater. **242** (2020). https://doi.org/10.1016/j.conbuildmat.2020.118098
4. Herle, I., Herbstová, V., Kupka, M., Kolymbas, D.: Geotechnical Problems of Cultural Heritage due to Floods. J. Perform. Constr. Facil. **24**, 446–451 (2010). https://doi.org/10.1061/(asce)cf.1943-5509.0000058
5. Trizio, F., Torrijo, F.J., Mileto, C., Vegas, F.: Flood risk in a Heritage City: Alzira as a Case Study. Water (Switzerland) **13**, 1138 (2021). https://doi.org/10.3390/w13091138
6. CRED: Human Cost of Disasters. An Overview of the Last 20 Years 2000–2019 (2020)
7. Eguibar, M.Á., García, R.P., Torrijo, F.J., Roca, J.G.: Flood Hazards in Flat Coastal Areas of the Eastern Iberian Peninsula: A Case Study in Oliva (Valencia, Spain). pp. 1–25 (2021)

8. Martínez-Gomariz, E., Forero-Ortiz, E., Guerrero-Hidalga, M., Castán, S., Gómez, M.: Flood depth-damage curves for Spanish urban areas. Sustainability **12** (2020). https://doi.org/10.3390/su12072666
9. Rudofsky, B.: Architecture without architects: a short Introduction to non-pedigreed architecture. Trad Sp. Arquitectura sin arquitectos : una breve introducción a la arquitectura sin pedigrí. Pepitas de Calabaza, Logroño (1964)
10. Mileto, C., López-Manzanares, F.V., Crespo, L.V., García-Soriano, L.: The influence of geographical factors in traditional earthen architecture: the case of the Iberian Peninsula. Sustainablity **11** (2019). https://doi.org/10.3390/su11082369
11. Drdácký, M.F.: Flood damage to historic buildings and structures. J. Perform. Constr. Facil. **24**, 439–445 (2010). https://doi.org/10.1061/(asce)cf.1943-5509.0000065
12. Hall, M., Djerbib, Y.: Moisture ingress in rammed earth: Part 1 - the effect of soil particle-size distribution on the rate of capillary suction. Constr. Build. Mater. **18**, 269–280 (2004). https://doi.org/10.1016/j.conbuildmat.2003.11.002
13. Morel, J.C., Bui, Q.B., Hamard, E.: Weathering and durability of earthen material and structures. In: Modern Earth Buildings: Materials, Engineering, Constructions and Applications. pp. 282–303. Woodhead Publishing (2012)
14. Miranda, F.N., Ferreira, T.M.: A simplified approach for flood vulnerability assessment of historic sites. Nat. Hazards **96**(2), 713–730 (2019). https://doi.org/10.1007/s11069-018-03565-1
15. Stephenson, V., D'Ayala, D.: A new approach to flood vulnerability assessment for historic buildings in England. Nat. Hazards Earth Syst. Sci. **14**, 1035–1048 (2014). https://doi.org/10.5194/nhess-14-1035-2014
16. Arrighi, C., Brugioni, M., Castelli, F., Franceschini, S., Mazzanti, B.: Flood risk assessment in art cities: the exemplary case of Florence (Italy). J. Flood Risk Manag. **11**, S616–S631 (2018). https://doi.org/10.1111/jfr3.12226
17. Figueiredo, R., Romão, X., Paupério, E.: Flood risk assessment of cultural heritage at large spatial scales: framework and application to mainland Portugal. J. Cult. Herit. **43**, 163–174 (2020). https://doi.org/10.1016/j.culher.2019.11.007
18. Ortiz, R., Ortiz, P., Martín, J.M., Vázquez, M.A.: A new approach to the assessment of flooding and dampness hazards in cultural heritage, applied to the historic Centre of Seville (Spain). Sci. Total Environ. **551–552**, 546–555 (2016). https://doi.org/10.1016/j.scitotenv.2016.01.207
19. Mileto, C., Vegas, F., García, L., Pérez, A.: Assessment of vulnerability of earthen vernacular architecture in the Iberian Peninsula to natural risks. Generation of an analysis tool. Int. J. Archit. Herit. **16**, 1–14 (2021). https://doi.org/10.1080/15583058.2021.1970284
20. Trizio, F., Garzón-Roca, J., Eguibar, M.Á., Bracchi, P., Torrijo, F.J.: Above the Ravines: flood vulnerability assessment of Earthen Architectural Heritage in Quito (Ecuador). Appl. Sci. **12**, 11932 (2022). https://doi.org/10.3390/app122311932
21. de Moel, H., Jongman, B., Kreibich, H., Merz, B., Penning-Rowsell, E., Ward, P.J.: Flood risk assessments at different spatial scales. Mitig. Adapt. Strat. Glob. Change **20**(6), 865–890 (2015). https://doi.org/10.1007/s11027-015-9654-z
22. Balasch, J.C., et al.: The extreme floods in the Ebro River basin since 1600 CE. Sci. Total Environ. **646**, 645–660 (2019). https://doi.org/10.1016/J.SCITOTENV.2018.07.325
23. Gobierno de Aragón: ANEXO I Municipios y núcleos de población situados en Zona A de alto riesgo, a efectos de emergencia para poblaciones, incluidos en el Anexo XII (tabla 12), del Decreto 201/2019, de 8 de octubre, del Gobierno de Aragón (2019)
24. Merz, B., et al.: Floods and climate: emerging perspectives for flood risk assessment and management. Nat. Hazards Earth Syst. Sci. **14**, 1921–1942 (2014). https://doi.org/10.5194/nhess-14-1921-2014
25. Confederación Hidrográfica del Ebro: Gestión de riesgos de inundación, https://www.chebro.es/web/guest/plan-de-gestion-de-riesgos-de-inundacion-segundo-ciclo

26. EC: DIRECTIVE 2007/60/EC OF THE EUROPEAN PARLIAMENT AND OF THE COUNCIL of 23 October 2007 on the assessment and management of flood risks (2007)
27. Mileto, C., Vegas López-Manzanares, F.: SOStierra. La restauración y rehabilitación de arquitectura tradicional de tierra en la Península Ibérica. Líneas guía y herramientas para una intervención sostenible, https://sostierra.blogs.upv.es/inicio/
28. Gordon, J.T.: The Delphi method. Futur. Res. Methodol. **16** (1994). https://doi.org/10.1007/BF02197902
29. Meyer, V., Haase, D., Scheuer, S.: Flood risk assessment in European river basins-concept, methods, and challenges exemplified at the Mulde river. Integr. Environ. Assess. Manag. **5**, 17–26 (2009). https://doi.org/10.1897/IEAM_2008-031.1
30. Dutta, D., Herath, S., Musiake, K.: A mathematical model for flood loss estimation. J. Hydrol. **277**, 24–49 (2003). https://doi.org/10.1016/S0022-1694(03)00084-2
31. Messner, F., et al.: Evaluating flood damages: guidance and recommendations on principles and methods (2007)
32. Kelman, I., Spence, R.: An overview of flood actions on buildings. Eng. Geol. **73**, 297–309 (2004). https://doi.org/10.1016/j.enggeo.2004.01.010